The 9th European Congress on Computational Methods in Applied Sciences and Engineering
ECCOMAS Congress 2024
3–7 June 2024, Lisboa, Portugal

STUDY ON THE EFFECT OF THE UPCOMING TURBULENT BOUNDARY LAYER ON AUTOMOTIVE TEST CASE ECCOMAS CONGRESS 2024

Andrew O'Sullivan[1], **Luca Mangani**[2] **AND Esteban Ferrer**[3]

[1,2] Cadence Design Systems,
Chaussée de la Hulpe 187, 1170 Brussels, Belgium
e-mail: oandrew@cadence.com, lmangani@cadence.com

[3] ETSIAE-UPM-School of Aeronautics,
Universidad Politécnica de Madrid,
Plaza Cardenal Cisneros 3, E-28040 Madrid, Spain
email: esteban.ferrer@upm.es

Key words: Computation Fluid Dynamics, CFD, Large Eddy Simulations, LES, Windsor Body, DrivAer, turbulent inflow generators

Summary. In the present study, we compare different strategies (Volume Forcing and Digital Filter) to simulate the upcoming turbulent boundary layer for LES codes on automotive test cases and quantify the impact. The test case is the yawed Windsor Body which is one of the two automotive benchmarks used for AutoCFD 3 and AutoCFD4 workshops and which has extensive experimental and previous CFD results to compare against. The upcoming turbulent boundary layer is of similar size as the gap between the bottom of the Windsor Body and the floor, making it thus a test case of interest to verify the sensitivity to the upcoming boundary layer. For the study, we use a low mach, Finite Volume Wall Modeled Large Eddy Simulation solver together with the turbulence generator strategies. We ran the test case not only at the operating condition of the AutoCFD workshop but verified the sensitivity to the upcoming boundary layer thickness and the inlet turbulence intensity. We analyse the effect on : the mean forces (drag and side force), the variance of the forces, frequencies of the force oscillations, wake structures and Cp profiles.

The goal is to understand which metrics are more sensitive to the CFD inlet settings such that this can be applied to other automotive test cases where the operating conditions (upcoming boundary layer) are either unknown or incomplete; and thus determine whether the upcoming boundary layer can explain the differences with experimental results on other test cases.

1 INTRODUCTION

In today's day and age, engineering design are being carried more and more numerically thanks to the increase in computational resources. For automotive aerodynamic applications, Computational Fluid Dynamics (CFD) has become the primary tool used for the design. However to validate the accuracy of the CFD it should be compared against experimental data (i.e. wind tunnel experiment). Many such CFD algorithms exist going from low fidelity steady state

RANS (Reynolds Averaged Navier Stokes) all the way to DNS (Direct Numerical Simulation) which resolved all the turbulent length and time scales. When discrepancies appear between the two, it becomes necessary to find the potential causes. Could it setup related, boundary conditions related, mesh related, solver related, time step related, etc. ? The AutoCFD workshop [2] was specifically setup to carry out this sort of investigations with multiple participants using different CFD solvers. With both a simplified model called the Windsor Body which was yawed to avoid bi-stability and a realistic car model called the DrivAer which was originally designed by TUM [1]. When carrying out benchmarking work previously on the yawed Windsor Body with our High Order LES code [6], we had noticed a strong under prediction of the drag coefficient (about 10%) similarly to other participants. This prompted questions about what might be the cause and one hypothesis put forward was that the effect of the upcoming boundary layer and turbulence intensity was non-negligible. In this case we therefore wish to understand what is the effect of the inlet profile/turbulence intensity on such automotive test cases. To verify this we use the Wall Modeled LES, low mach CharLES solver [7] together with two of turbulence inflow generator strategies implemented in the code : the Volume Forcing approach and the Digital Filter approach. This is particular might be useful for test cases, where the operating conditions are unknown or incomplete and thus allow us to understand the sensitivity the different metrics to the inlet operating conditions.

2 TEST CASES

For this study, we use two automotive test cases used for benchmarking CFD solvers at the AutoCFD workshop [2]. Since the workshop provides mesh settings and experimental data we thus carry out a comparison with both simulations and experiment.

2.1 Yawed Windsor Body

The first case is the yawed Windsor Body, which is a simplified body similar to the Ahmed body. The yawed test case was introduced during the third edition of the workshop to avoid bi-stability issues encountered during the first two editions. The Windsor body as shown in Fig. 1 is yawed by 2.5° and placed inside a domain a length 11m, width 1.92m and 1.32m high.

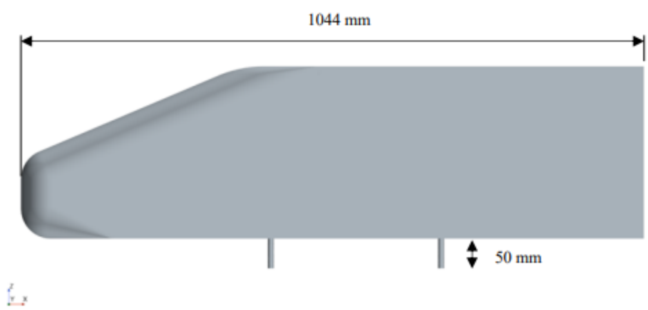

Figure 1: Windsor Body [3]

The boundary conditions are defined by the workshop as follows : floor (no slip), ceiling, side walls (), body (no slip), outlet (pressure outlet), inlet ($U_{\text{inf}} = 40$m/s)

2.2 DrivAer NotchBack

In order to validate the findings from the Yawed Windsor Body test case, a second realistic automotive test case was chosen : the DrivAer Notchback model. The original DrivAer model [1] was designed by the *Technical University of Munich* back in 2011. The one used in this study is the Notchback version used in the AutoCFD4 workshop shown in Fig. 2 but with closed cooling. Experimental data was collected in the Pininfarina windtunnel.

Figure 2: DrivAer Notchback [4]

The boundary conditions are kept the same as defined in the workshop with slip side walls, a slip floor upstream and a moving floor under the car (see [4] for exact dimensions).

3 SOLVER

For the present test cases, we use the low mach Finite Volume Wall Modeled LES CharLES code. This solvers allows us to run LES automotive simulations without having the same computational restrictions as Wall Resolved LES. The usage of an algebraic wall model is well suited for turbulent boundary layer which is what we generally expect to find on most automotive test cases. Should the boundary layer physics be more complex (e.g. laminar to turbulent transition, laminar separation bubbles), we recently showed that the solver with the wall model can account for all these more complex physics provided the mesh resolution is sufficient [7].

Two different turbulent inflow generation strategies are present in the code, which are compared in the results :

- The Volume Forcing approach : The main idea here is to add a source term to the 3 momentum Navier Stokes equations within a user define box.
  - Advantage : The forcing box can be places anywhere in the domain.
  - Disadvantage : Cannot control explicitly the turbulent length scales being generated.
- The Digital Filter approach : For each velocity component a random perturbation is created on a 2D cartesian grid. The perturbations are then correlated to their spatial neighbours with a filtering operator that depends on the target turbulent length scale set by the user. Temporal correlations must also be taken into account between time steps.
  - Advantage : Can manually set a target turbulent length scale (Integral length scale)

- Disadvantage : Must be placed at the inlet. This means that the mesh upstream must be kept refined upstream of the body to avoid the inlet turbulence being too dissipated by the time it reaches the vehicle. Creates large nonphysical pressure oscillations.

4 MESH SETUP

The AutoCFD workshop already provided ANSA meshes in order to provide consistency for all the participants (see Mesh parameters in the Appendix). Since the CharLES solver relies on a internal Vornoi mesh generator called *stitch*, we therefore reproduced the intermediate G2 mesh with our internal mesh generator as shown in Fig. 3. The background base mesh size is two levels more refined in order to preserve the upstream turbulence form the inlet.

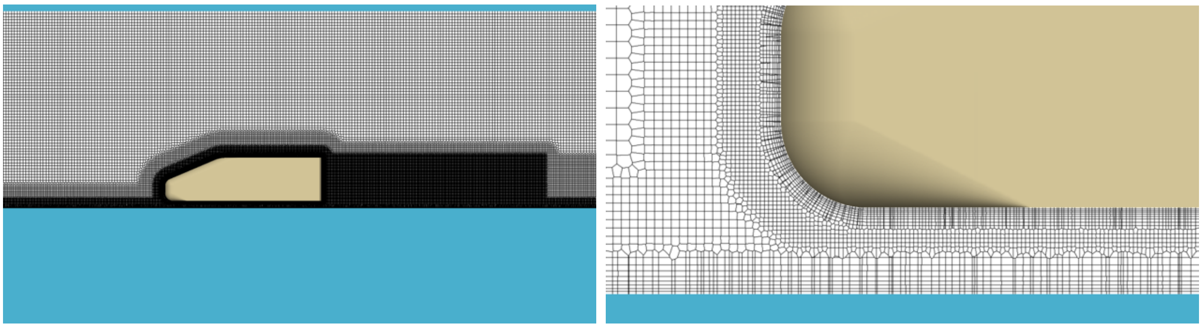

(a) Mesh with workshop refinement boxes (b) Structured boundary layer

Figure 3: Symmetry Plane slices of the mesh

This resulted in a mesh with approximately 37 million cells for the Yawed Windsor Body and a mean y^+ on the surface of the body around 30 (see Fig. 4). This is generally the recommended value for algebraic wall model with turbulent boundary layers.

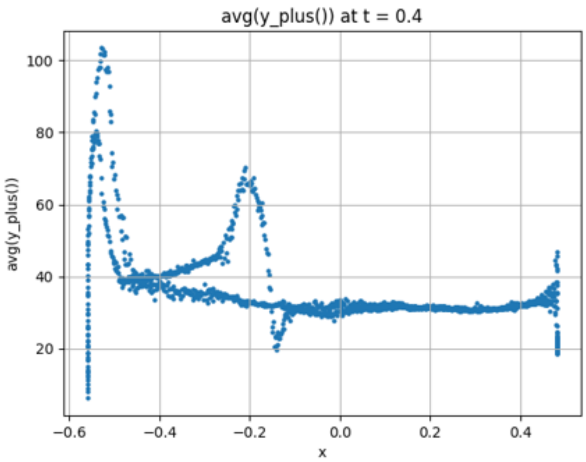

Figure 4: Mean y^+ along the symmetry slice

5 Results

Before running the simulations on the Windsor Body, we ran some tests on an empty wind tunnel case with the same mesh parameters. As stated previously, with the Volume Forcing approach we cannot control the integral length scale. We therefore carried out a test and measured the integral length scale at several point in the domain and found an integral length scale of about 5cm. This is then used a one of the target integral length scales for the Digital Filter approach.

5.1 Windsor Body

5.1.1 Forces

The first metric we use to compare the different inlet settings is the integrated forces (drag and side force). In Fig. 5a we compare the drag coefficient signal of the baseline simulation with both the digital filter approach and the volume forcing approach. As can be seen by the mean values reported in the legend, the mean values remain close to each other for all the simulations (3.5% relative difference), however we can notice that the fluctuation amplitude vary far more significantly. In particular, the Digital Filter with large integral length scale (L $\approx$ 1m) has a standard deviation about 3 time larger than the simulations ran with the volume forcing approach. All the LES simulations appear to underestimate the drag coefficient by about 10% which is consistent with the finding from the previous AutoCFD Workshops results, which also run the same CFD setup. This might potentially indicate that the domain setup doesn't match the wind tunnel well (e.g. blockage ratio insufficient for a yawed case with yawed wake and slip side walls). For the side force signal a similar trend can be observed, with the mean force not been significantly impacted but even more significant impact coming from the by the usage of the Digital Filter which allows for larger integral length scales. In this case the standard deviation increases by a factor 10x. This appears to indicate that large areas of low and high pressure that are of similar size as the vehicle move around the sides of the vehicle causing significant fluctuations.

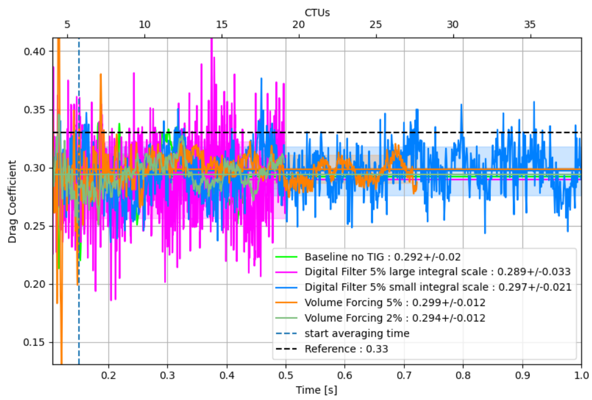

(a) Drag Coefficient Signal

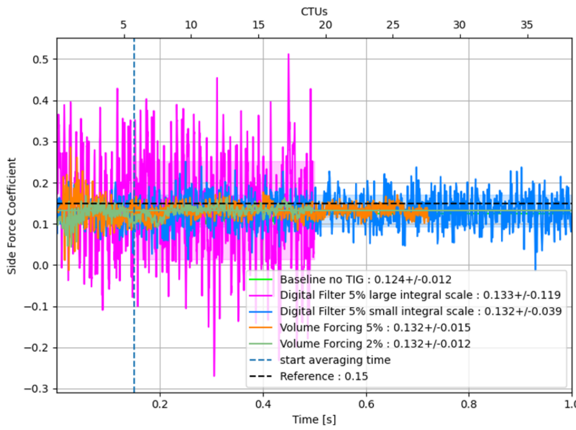

(b) Lift Coefficient Signal

Figure 5: Integrated Forces Signal

The following conclusions can be made from the analysis of the integrated forces

- Mean forces are not impacted by increasing the turbulence intensity or changing the correlation length / integral length scale
- Standard deviation of the forces is not impacted by increasing the turbulence intensity at the inlet. It is however impacted by increasing the integral length scale once the integral length scale is of the same order of magnitude as the length of the body over which we are integrating the forces.
- The Digital Filter approach generated larger fluctuations of the integrated forces than the Volume Forcing approach for the same turbulence intensity and the same integral length scale.

5.1.2 Cp Profiles

Integrated forces can be correct but for the wrong reason, since two inaccuracies might cancel each other out when integrating over a surface. This can lead us to believe that the CFD is giving good results despite actually being inaccurate. Since pressure forces are the dominant force on bluff body shapes such as the Windsor Body, comparing the non-dimensional pressure coefficient around the body is a far better metric to assess the accuracy of the CFD results.

For the workshop, three different slices on which experimental data is collected are given :

- Symmetry Plane : $y_{WB,ref} = 0$
- Bumper Slice : $z = 0.1249$
- Shoulder Slice : $z = 0.2595$

In Fig. 15 we see the time averaged C_p profile on both the symmetry plane and the shoulder slice for the various simulations and observe no impact coming from the various inlet settings except for the backface. We also observe that the C_p profile generally agrees well with the experimental data points except on the lefthand side of the shoulder slice. This is however an observation also seen by other CFD simulations [5]. This is unsurprising since the mean forces were not significantly impacted by the turbulent inlet conditions.

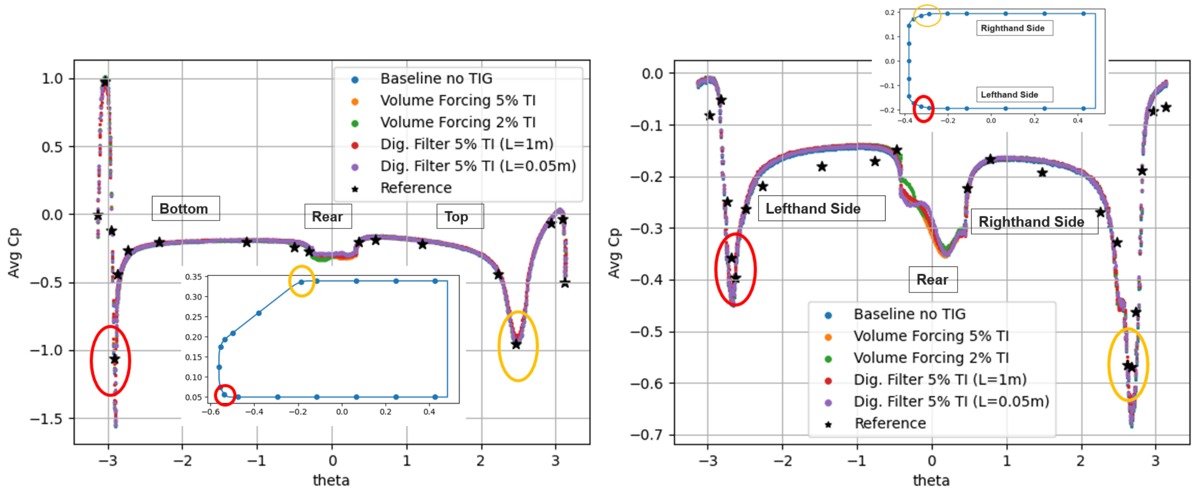

(a) Symmetry Plane

(b) Shoulder Slice

Figure 6: Average pressure coefficient C_p

Lets us now however take a look at the RMS values of C_p. In Fig. 7 we illustrate how the C_p RMS is impacted around the symmetry plane by the different turbulent inlet settings. However while the RMS increases with the increase of the turbulence intensity, these perturbation remain local (integral length of 5cm). Once we average out over the whole body these fluctuations cancel each other out which explains why the standard deviation was not too impacted by increasing the turbulence intensity. But once we use the Digital filter with large integral length scale these fluctuations do not average each other out over a single time step, thus explaining the dramatic increase in the standard deviation of the integrated forces seen previously.

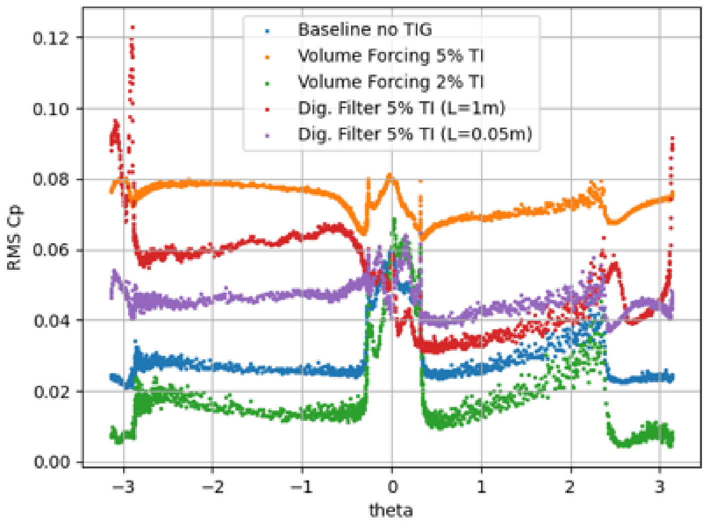

Figure 7: Symmetry Plane : Cp RMS

The following conclusions can be made from the analysis of the C_p profiles :

- The turbulent inlet conditions do no impact the mean C_p profile on the surface of the body. Hence why the mean forces were not impacted.
- The C_p RMS does appear to have been impacted by increasing the turbulence intensity, except the 2% volume forcing which appears to be an outlier.
- For the same turbulence intensity, the Digital Filter produces larger pressure fluctuations than the Volume Forcing approach.

5.1.3 Cf Profiles

Similarly to the pressure coefficient, skin friction C_f data is also collected and compared on the same three slices. However, unlike for C_p no experimental data to compare against is given.

In Fig. 8, we compare the average skin friction coefficient C_f on the symmetry plane. As can be noted, no noticeable difference between the five simulations can be seen. The other two slices are added in the Appendix since the differences remain negligible.

We thus conclude by stating the mean skin friction is not impacted by increasing the inlet turbulence intensity or the correlation length.

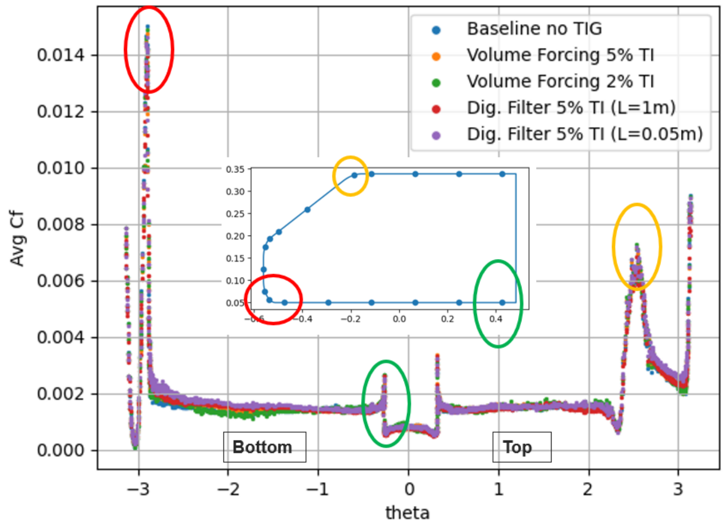

Figure 8: Average C_f on the symmetry plane. No significant different caused by inlet conditions.

5.2 Point Probes

Having analysed the C_p and C_f profiles on the surface of the Windsor Body, let us now look more in detail at any potential differences of the physics at the surface of the body. The experimental results given by the workshop give a set of pressure taps on the surface of the body. We therefore use these locations to measure the local pressure and velocity oscillations in time in order to get further information. The experimental probe location given by the workshop are projected onto the nearest cell centroid. Therefore the fluctuations in time tell us how C_p varies in time, while the velocity probe data tell us how C_f varies in time locally.

Firstly, let's compare the velocity spectrum and probability distribution at a single probe location at top of the vehicle. This comparison is shown in Fig. 9 where we compare the energy spectrum of the U_x component of velocity at tapping probe 15 near at the rear of the roof of the WindsorBody. As can seen, both the spectrum and the histogram does not appear to be affected y the choice of the turbulent inlet conditions. We also clearly observe the -5/3 power law when looking at the energy cascade. We can thus clearly see that the BL is turbulent and how much of the energy spectrum is resolved (until about St = 30 or about 1000 Hz) and how much is dissipated (beyond approx 1000 Hz) either numerically because of the mesh resolution or simply because of physical viscosity is dominate (i.e a DNS mesh). In this case it is dissipated numerically since we are using WMLES in the boundary layer.

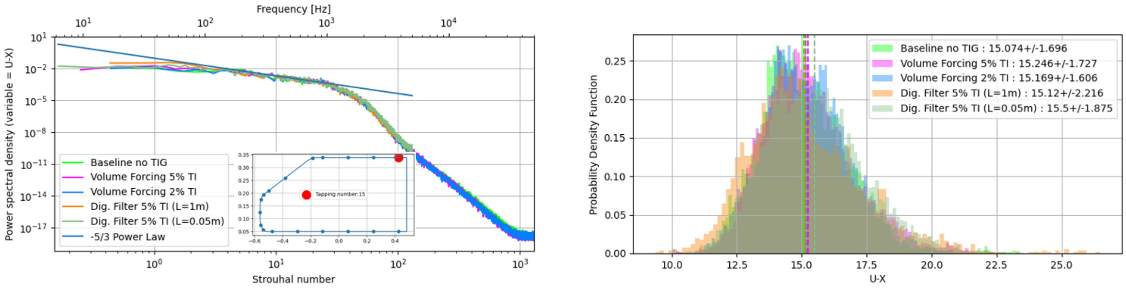

(a) Energy spectrum of U_x velocity component. -5/3 power law is present thus indicating a turbulent boundary layer

(b) Probability distribution : inlet TI does not impact the mean or the distribution of the near wall velocity

Figure 9: Analysis of the U_x velocity component at tapping probe 15 on the top rear of the body.

The following conclusions can be made from the analysis of the surface point probe data :

- Almost all of the velocity probes have the characteristics of a turbulent flow : energy cascade with -5/3 power law, an autocorrelation function with an exponential decay over short correlation times.
- The velocity turbulent characteristics are not impacted by increasing the turbulence intensity or changing the integral length scale. It appears as though the physics of the eddies at the first cell height is not impacted by the perturbations happening in the outer field.
- The pressure probes have different characteristics in terms of energy spectrum, autocorrelation, etc... (see Fig. 14 in Appendix)
- We notice that the variance of pressure increases as we increase the inlet turbulence intensity. This can be explained by the fact that the pressure in the wall normal direction is almost constant. Therefore the pressure at the wall feels the effect of the pressure fluctuations further away from the body. Unlike for velocity, for which these fluctuations get diffused in the boundary layer.

5.3 DrivAer Notchback

To validate the findings on the Yawed WindsorBody, a quick comparison was carried out between the baseline case (no turbulent inflow) and the Volume Forcing approach with 2% turbulent intensity.

Firstly we once verified the effect on the integrated forces. As is shown in Fig. 10 no impact can be seen on the mean drag coefficient, the standard deviation or the spectrum. This is consistent with the Windsor Body, where the noticeable differences appeared when the target integral length scale became of similar size as the vehicle.

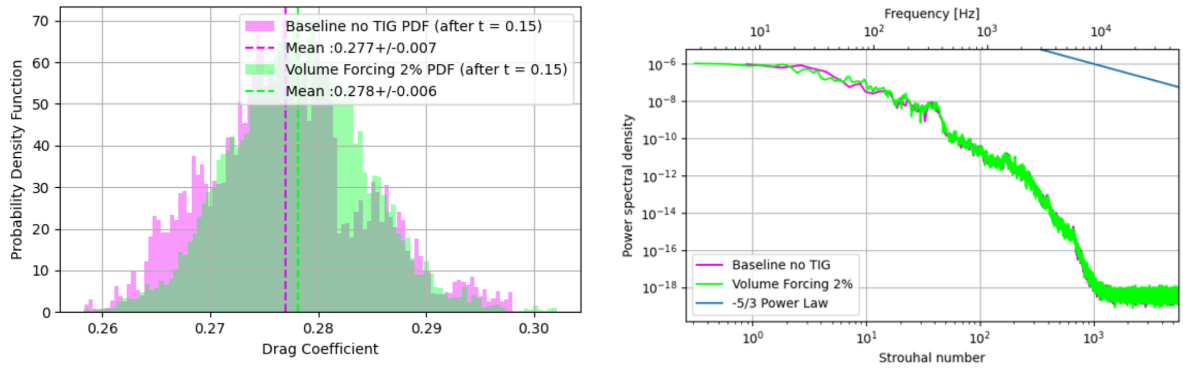

(a) Histogram (b) Spectrum

Figure 10: Drag Coefficient

Finally we compare the centerline mean C_p profile over the top of the car from the bumper, over the hood, all the way to the rear number plate. As can once again be seen in Fig 11 the mean C_p profile is not affected by the turbulence intensity at the inlet. It also agrees very well with the experimental reference probes. Thus indicating that the choice of the algebraic wall model seems well suited for this test case with $y^+ > 30$.

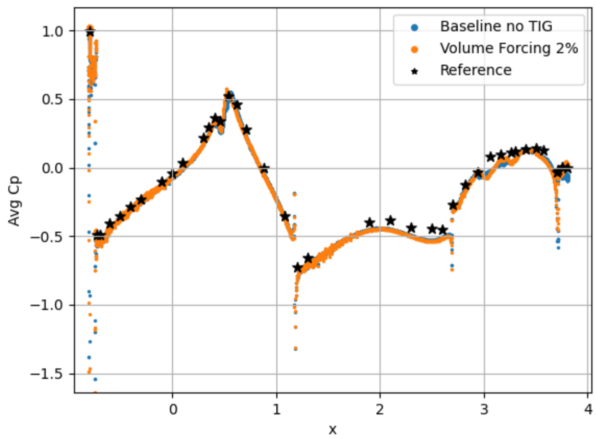

Figure 11: Mean C_p over the top of the DrivAer Notchback

6 CONCLUSIONS

In this study, we compared two different turbulent inflow generators (Volume Forcing and Digital Filter) with a baseline simulation that has constant inlet velocity. We were able to verify the effect of the turbulence intensity and the integral length scale on two automotive benchmarks from the AutoCFD Workshop: the yawed Windsor Body and the DrivAer Notchback. We demonstrated that the turbulence intensity did not impact the mean or the standard deviation of the integrated forces. The main impact arose when we set a integral length scale that was of a similar size as the vehicle over which we integrate the forces. We also observed that the mean pressure coefficient C_p and skin friction coefficient C_f profiles were not affected by any of the inlet settings. Only the RMS appear to be affected the inlet conditions (C_f RMS was not measured). When looking a point probes within the boundary layer, we observe that both the histogram and the energy spectrum of velocity probes was not affected (-5/3 power law clearly visible in Fig. 9). This implies that the C_f RMS is also not affected and that the velocity properties of the inner turbulent boundary layer are not affected by the fluctuations in the outer field. The velocity field inside the inner part of a turbulent boundary layer is not affected by the far field fluctuations, however the pressure inside the a turbulent boundary layer is affected since pressure is almost constant in the wall normal direction.

Future developments that allow the Volume Forcing approach to set a target integral length scale are underway. This would make the Volume Forcing approach the clear choice of turbulent inflow generators since we saw the impact that the integral length scale can have.

Appendix

Table 1: Grid Parameters

Component	Description	Item	g1 (coarse)	g2 (baseline)	g3 (fine)
Car	Surface	Size (m)	4.8×10^{-3}	2.4×10^{-3}	1.32×10^{-3}
	Shoulder/pin	Size (m)	2.4×10^{-3}	2.4×10^{-3}	1.32×10^{-3}
	Prism Layer	Number	9	9	9
		Thickness* (m)	0.0144	0.01194	0.01382
		Near wall size (m)	0.7×10^{-3}	0.7×10^{-3}	0.7×10^{-3}
Ground plane	Surface	Min Size (m)	0.096	0.048	0.0264
	Prism Layer	Number	9	9	9
		Thickness (m)	0.04	0.04	0.04
		Near wall size (m)	1.5×10^{-3}	1.5×10^{-3}	1.5×10^{-3}
Under car/wake	Surface	Min Size (m)	4.8×10^{-3}	2.4×10^{-3}	1.32×10^{-3}
	Prism Layer	Number	9	9	9
		Thickness (m)	0.013	0.013	0.013
		Near wall size (m)	1.0×10^{-3}	1.0×10^{-3}	1.0×10^{-3}
Wake Refine	Near	Extent x= (m)	0.48-2.0	0.48-2.0	0.48-2.0
		Size (m)	4.8×10^{-3}	2.4×10^{-3}	1.32×10^{-3}
	Far	Extent x= (m)	2.0-3.0	2.0-3.0	2.0-3.0
		Size (m)	9.6×10^{-3}	4.8×10^{-3}	2.64×10^{-3}
Number of Cells			**6.31×10^{6}**	**37.3×10^{6}**	**197.5×10^{6}**

Figure 12: ANSA Mesh Parameters [3]

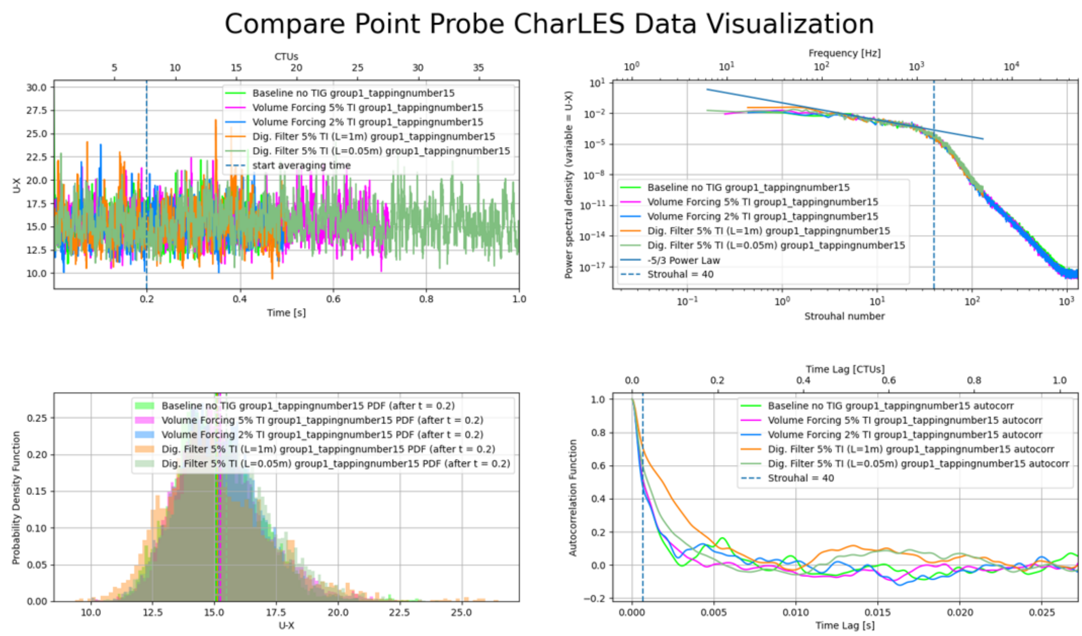

Figure 13: Probe 15 : Velocity Analysis. No significant impact from the inlet conditions. C_f RMS most likely not affected.

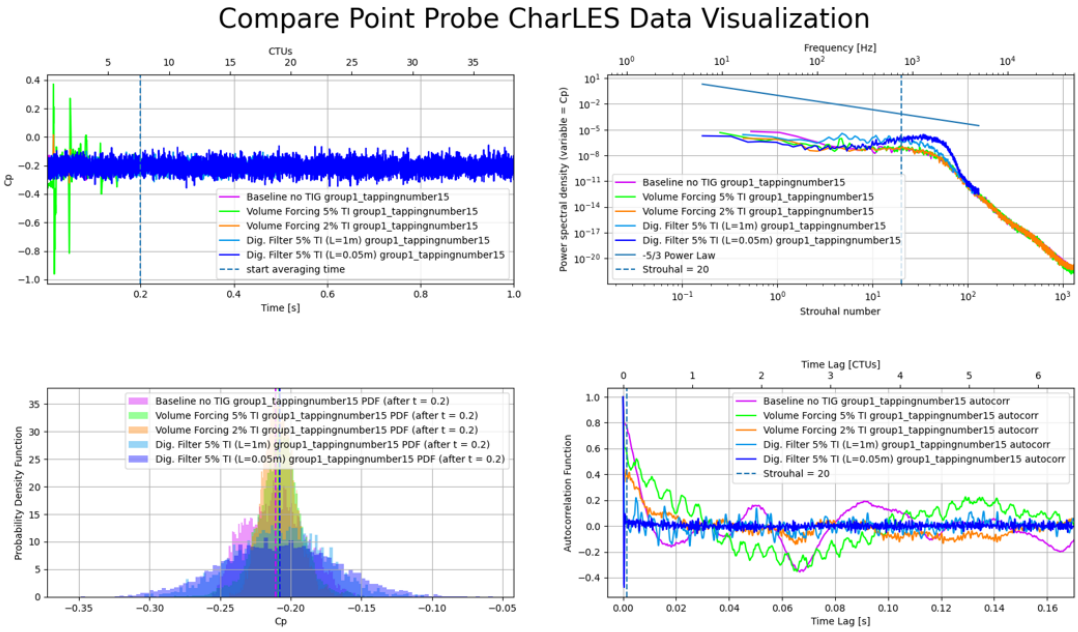

Figure 14: Probe 15 : Pressure Analysis. Pressure is affected by turbulent inlet conditions.

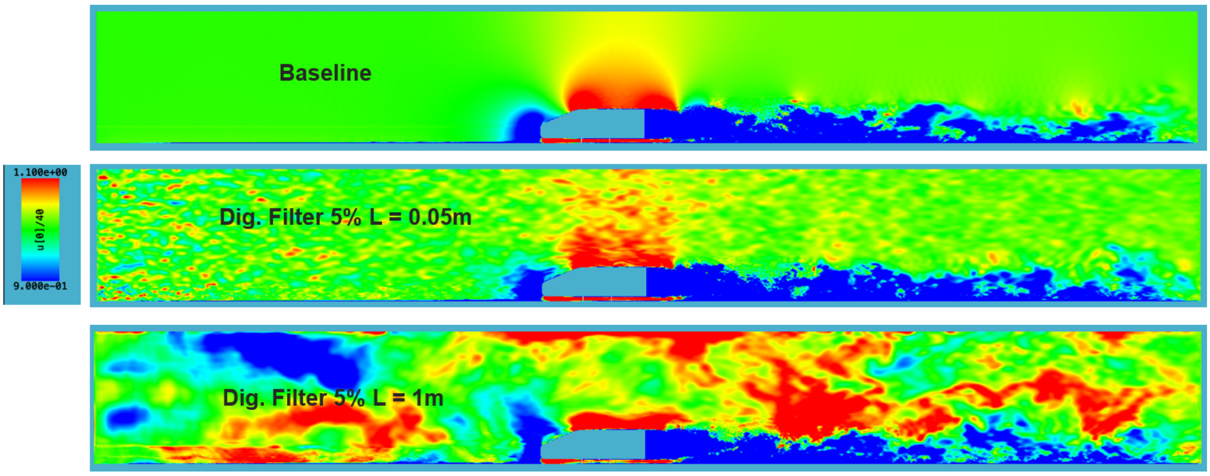

Figure 15: Illustrating the effect of the integral length scale at the inlet on the instantaneous velocity field.

REFERENCES

[1] Chair of Aerodynamics and Fluid Mechanics Technical Univeristy of Munich, "DrivAer Model", https://www.epc.ed.tum.de/en/aer/research-groups/automotive/drivaer/

[2] AutoCFD4, "4th Automotive CFD Prediction Workshop", https://autocfd.org/

[3] Page Garry, "4th Automotive CFD Prediction Workshop Case 1: Windsor Squareback at Small Yaw Case Description", https://autocfd4.s3.eu-west-1.amazonaws.com/test-cases/case1/Gary+Page+-+Case1AutoCFD4Description.pdf

[4] Hupertz B, "AutoCFD4 – Test Case 2a/b : DrivAer - Notchback", https://autocfd4.s3.eu-west-1.amazonaws.com/test-cases/case2/AutoCFD4_Case2_Intro_240409.pdf

[5] AutoCFD Workshop, "3rd Automotive CFD Prediction Workshop", https://auto-cfd-workshop-3.cfdsolutions.net/

[6] Charles Hirsch and Koen Hillewaert and Ralf Hartmann and Vincent Couaillier and Jean-Francois Boussuge and Frederic Chalot and Sergey Bosniakov and Werner Haase, "TILDA: Towards Industrial LES/DNS in Aeronautics", In Springer, 2021, https://link.springer.com/book/10.1007/978-3-030-62048-6

[7] O'Sullivan Andrew, Puri Kunal and Ferrer Esteban, "Best Practices and Mesh Convergence on the Extruded Imperial Front Wing With CharLES Solver", AIAA Conference 2024, 2024, https://arc.aiaa.org/doi/10.2514/6.2024-4259